Endohedral Fullerenes

DOI: 10.1002/anie.200703489

The Large $Nd_3N@C_{2n}$ ($40 \leq n \leq 49$) Cluster Fullerene Family: Preferential Templating of a C_{88} Cage by a Trimetallic Nitride Cluster**

*Frederic Melin, Manuel N. Chaur, Sarah Engmann, Bevan Elliott, Amar Kumbhar, Andreas J. Athans, and Luis Echegoyen**

The field of trimetallic nitride endohedral fullerenes began in 1999 with the discovery of $Sc_3N@C_{80}$ by Dorn and co-workers.[2] They vaporized graphite rods packed with scandium oxide in a Kratschmer–Huffman arc reactor under a mixture of nitrogen and helium. Later, Dunsch and co-workers showed that the same compound can be obtained in higher yields under a mixture of helium and ammonia.[3] Scandium is the smallest metal that has been shown to form a trimetallic nitride cluster inside a fullerene. The conditions described by Dunsch et al. afford mainly $Sc_3N@C_{80}$ in high yields, as compared to reported mono-, di-, or trimetallofullerenes,[1] along with small amounts of $Sc_3N@C_{68}$ and $Sc_3N@C_{78}$ (Figure 1, top HPLC trace). Over the years, the family of trimetallic nitride endohedral fullerenes has been considerably expanded with the encapsulation of a new Group 3 metal (Y),[3] lanthanides (Er,[2] Ho,[3,8] Lu,[4] Tm,[5] Gd,[6,7] Dy,[9] Tb[8,10]), and mixed metal clusters.[2,11] Upon increasing the size of the encapsulated metal (from Sc to Gd), the yield of cluster fullerenes usually decreases, and a distribution of molecules is obtained, with cages as big as C_{88}. The C_{80} cage, however, remains the most abundant. For instance, the $Y_3N@C_{2n}$ family consists mainly of $Y_3N@C_{80}$ along with small amounts of $Y_3N@C_{82}$, $Y_3N@C_{84}$, $Y_3N@C_{86}$, and $Y_3N@C_{88}$ (Figure 1, middle trace; for MALDI data, see the Supporting Information). Dysprosium gives the largest distribution of molecules reported to date, the smallest cage produced being C_{76} and the largest C_{98}.[9] In the case of Gd_3N, which is the largest cluster encapsulated to date, no cage smaller than C_{80} is obtained, and the relative abundance of the bigger cages (C_{82}, C_{84}, C_{86}, and C_{88}) is higher than that obtained with the other metals.[7]

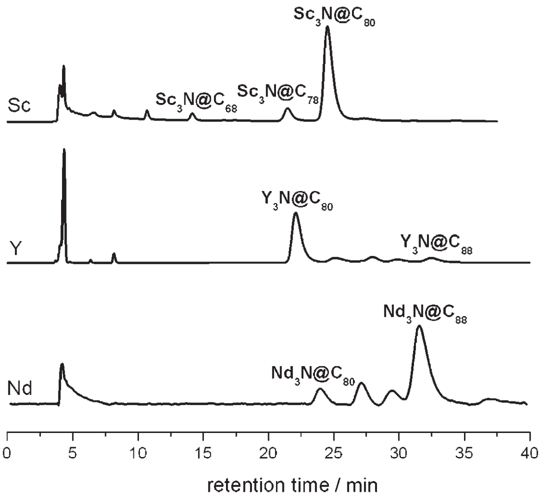

Figure 1. HPLC traces of the $Sc_3N@C_{2n}$, $Y_3N@C_{2n}$, and $Nd_3N@C_{2n}$ families obtained by arc burning graphite rods containing 10% metal oxide in a mixture of ammonia (20 mbar) and helium (200 mbar); column: 10×250 mm Buckyprep-M; eluent: toluene; flow rate: 4 mL min^{-1}; detection at 372 nm.

Calculations and experimental observations have given insight into the exceptionally high abundance of the C_{80} cage, which is observed even with clusters as large as Gd_3N. Poblet and co-workers linked this stability to a large HOMO–LUMO gap and have calculated that among all fullerenes that satisfy the isolated pentagon rule (IPR) from C_{60} to C_{84}, C_{80}:7 (I_h) and C_{80}:6 (D_{5h}) provide the largest HOMO–LUMO gap after encapsulating a trimetallic nitride cluster.[12] Raman and IR spectroscopy studies have also shown that a mutual stabilization of the cluster and the C_{80} cage through cluster–cage charge transfer could explain the high abundance of this cage.[7,13] However, the stabilization of cages bigger than C_{80} with clusters larger than Gd_3N cannot be ruled out. No reports of the encapsulation of larger clusters, such as La_3N, inside fullerene cages have appeared in the literature to date.

Herein, we report the preparation of $Nd_3N@C_{2n}$ ($40 \leq n \leq 49$) and the predominance of the larger C_{88} cage. These endohedral fullerenes were obtained by arc burning of high-purity graphite rods containing neodymium oxide under a mixture of ammonia (20 mbar) and helium (200 mbar). Rods containing 10% Nd_2O_3 seemed to give the best yield (0.2 mg per rod) of $Nd_3N@C_{2n}$ in the soluble extract of the soot. The new family of cluster fullerenes was characterized by mass spectrometry and HPLC. The most abundant species ($Nd_3N@$

---

[*] Dr. F. Melin, M. N. Chaur, S. Engmann, B. Elliott, Dr. A. J. Athans, Prof. Dr. L. Echegoyen
Chemistry Department, Clemson University
219 Hunter Laboratories, Clemson, SC 29630-0973 (USA)
Fax: (+1) 864-656-6613
E-mail: luis@clemson.edu

A. Kumbhar
Advanced Materials Research Laboratories
91 Technology Dr., Anderson, SC 29625 (USA)

[**] Financial support from the National Science Foundation to A.J.A. and L.E. (Grant number CHE-0509989) is greatly appreciated. This material is based on work supported by the National Science Foundation while L.E. was working there. All opinions, findings, conclusions, or recommendations expressed herein are those of the authors and do not necessarily reflect the views of the National Science Foundation. The authors also gratefully thank Greg Becht and Prof. Shiou-Jyh Hwu for their help in the annealing of the composite rods.

Supporting information for this article is available on the WWW under http://www.angewandte.org or from the author.

C_{88}) was also studied by UV/Visible/NIR spectroscopy and electrochemistry.

While five distinct peaks in the range 20–40 min can be seen in the HPLC trace (Figure 1, bottom), MALDI-TOF mass spectrometry analysis reveals the presence of at least ten different compounds in this family (Figure 2), with cages ranging from C_{80} to C_{98} and the highest peak corresponding to $Nd_3N@C_{88}$. The identity of the peaks observed in the HPLC trace was established by MALDI-TOF mass spectrometry analysis after isolation (Figure 3).

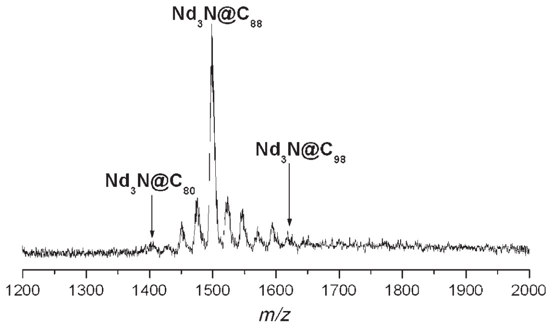

Figure 2. MALDI-TOF mass spectrum of the crude mixture of $Nd_3N@C_{2n}$.

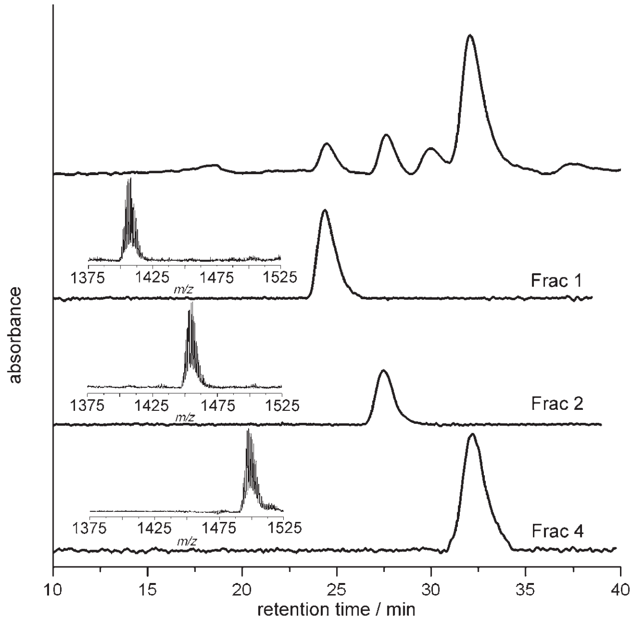

Figure 3. Chromatograms and MALDI-TOF mass spectra of $Nd_3N@C_{80}$ (fraction 1), $Nd_3N@C_{84}$ (fraction 2), and $Nd_3N@C_{88}$ (fraction 4). The top trace shows the unseparated mixture.

The compound with a retention time of 24 min (fraction 1) can be identified as $Nd_3N@C_{80}$. Its retention time is comparable to that of $Sc_3N@C_{80}$ (24.7 min). The second peak in the HPLC trace (retention time 27.1 min, fraction 2) can be attributed to $Nd_3N@C_{84}$. The fourth and highest peak (retention time 31.6 min, fraction 4) corresponds to $Nd_3N@C_{88}$. Its retention time is close to that of $Y_3N@C_{88}$ (32.7 min). Both the HPLC trace and MALDI-TOF spectra show that it is the most abundant species in the soluble extract of the arcing soot. The amount of material collected after isolation of each fraction confirmed that $Nd_3N@C_{88}$ is the most abundant species. A sample of this compound was also deposited on a TEM grid and submitted to an energy dispersive spectroscopy (EDS) analysis. The spectrum shows the characteristic peaks of neodymium (see the Supporting Information). The compound corresponding to the third peak in the HPLC trace was more difficult to isolate in pure form, owing to the close proximity of its retention time to the most abundant species. It can be tentatively assigned as $Nd_3N@C_{86}$. The fifth peak of the HPLC trace (retention time 36 min) has not been characterized, owing to its very low intensity.

Although neodymium is only slightly larger than gadolinium (Table 1), these studies show that the cage-size distributions of $Gd_3N@C_{2n}$ and $Nd_3N@C_{2n}$ are dramatically different. C_{88} is the most abundant species (relative yield 30–40 % as established by HPLC) in the case of neodymium, whereas the C_{80} cage is still predominant for gadolinium (relative yield 35–40 %).[7] However, the relative abundance of the other cages encapsulating these two clusters (the smaller cages C_{80}, C_{84}, and C_{86} for neodymium and the bigger cages C_{82}, C_{84}, C_{86}, and C_{88} for gadolinium) is far from negligible. It appears that the cluster Gd_3N is the upper threshold for stabilization of the C_{80} cage and that, similarly, the Nd_3N cluster is the lower threshold for stabilization of the C_{88} cage. Interestingly, the yield of $Nd_3N@C_{2n}$ (0.2 mg per rod) was found to be higher than those of $Y_3N@C_{2n}$ and $Gd_3N@C_{2n}$ and slightly less than that of $Sc_3N@C_{80}$ (0.3 mg per rod). The possibility to accommodate the Nd_3N cluster in bigger cages than the Gd_3N cluster apparently results in higher yields.

Table 1: Size of the metallic ion M^{3+} (octahedral coordination)[14] and of the cluster M_3N for some Group 3 and lanthanides elements.

Metal M	Sc	Y	Dy	Gd	Nd	La
$r(M^{3+})$ [Å]	0.75	0.90	0.91	0.94	0.98	1.05
$d(M_3N)$ [Å][a]	3	3.6	3.64	3.76	3.92	4.20

[a] Calculated using the literature formula $d(M_3N) = 4\,r(M^{3+})$.[7]

Owing to its relatively high yield, $Nd_3N@C_{88}$ could be easily isolated in high purity (greater than 95 %, see Figure 3) and in amounts allowing characterization by UV/Vis/NIR spectroscopy (see Figure 4 and the Supporting Information) and electrochemistry (Figure 5). The $Nd_3N@C_{88}$ spectrum shares some common characteristics with another trimetallic nitride cluster encapsulated in a C_{88} cage (Table 2). The band gap obtained from the spectral onset is comparable to that of $Dy_3N@C_{88}$[9] and is significantly lower than that usually obtained for the trimetallic nitride clusters encapsulated in C_{80} cages. $Nd_3N@C_{88}$ also presents two absorptions in the NIR region; such behavior was previously observed only for the C_{88} cage in the $Dy_3N@C_{2n}$ family.

The cyclic voltammogram of $Nd_3N@C_{88}$ was recorded in *o*-dichlorobenzene (*o*-DCB) containing 0.05 M $[NBu_4][PF_6]$ as

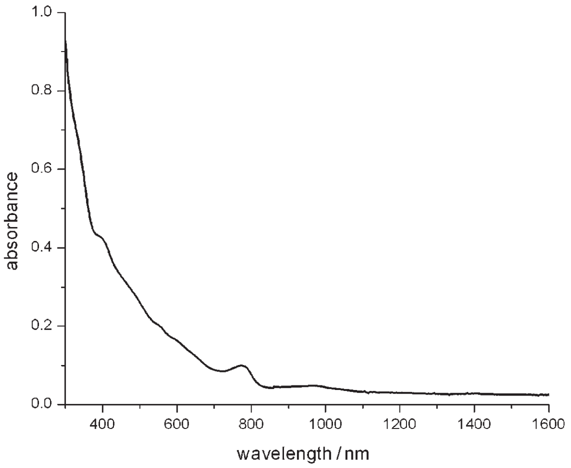

Figure 4. UV/Vis/NIR spectrum of $Nd_3N@C_{88}$ in toluene.

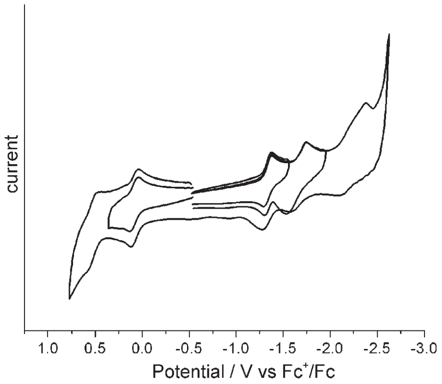

Figure 5. Cyclic voltammogram of $Nd_3N@C_{88}$ in $[NBu_4][PF_6]$/*o*-DCB with ferrocene as the internal standard; scan rate 100 $mV\,s^{-1}$.

Table 2: Comparison of the spectral characteristics of $Dy_3N@C_{88}$ and $Nd_3N@C_{88}$.

TNT EMF[a]	Onset [nm]	Band gap[b] [eV]	UV/Vis/NIR peaks [nm]
$Dy_3N@C_{88}$	1548	0.80	345, 733, 1045, 1462
$Nd_3N@C_{88}$	1420	0.87	390, 770, 965, 1400

[a] Trimetallic nitride template endohedral metallofullerene. [b] Calculated from the onset: (band gap in eV) ≈ 1240 (onset in nm)$^{-1}$.[9]

the supporting electrolyte and using a 2-mm-diameter glassy carbon disk as the working electrode. Three cathodic waves could be observed; the first was monoelectronic and reversible, while the second was monoelectronic and quasi-reversible. The third wave was less well defined and could be multielectronic. Anodically, the compound showed two waves; the first was monoelectronic and reversible, but the second was not very well defined. The redox behavior of $Nd_3N@C_{88}$ is significantly different from that of the reported nonderivatized $M_3N@C_{80}$ species, which always showed irreversible reduction steps in *o*-DCB.[15] The electrochemical HOMO–LUMO gap obtained for $Nd_3N@C_{88}$ (1.40 V) is also significantly smaller than that usually obtained for $M_3N@C_{80}$ (greater than 1.80 V, see the Supporting Information).[15]

In conclusion, the new $Nd_3N@C_{2n}$ family of trimetallic nitride fullerenes shows very interesting features and gives answers to several questions concerning the influence of the size of the encapsulated cluster on the yield of endohedral fullerenes and the cage-size distribution. The limit of stability of the C_{80} cage is now reached, since the cluster Nd_3N prefers to be encapsulated in the small-band-gap C_{88} cage. Interestingly, the transition between the predominance of the C_{80} cage, which is still observed for Gd_3N, and the predominance of the C_{88} cage, which is observed for the first time with Nd_3N, comes with an increase in the yield of production. Additional studies are underway to determine the structure of $Nd_3N@C_{88}$. There are 35 possible IPR isomers for the C_{88} cage, but as in the case of terbium, only one might be obtained.[10] It is also interesting to determine the geometry of the encaged cluster, which has been shown to depend on the relative size of the cluster and the cage.[16] Such a stable and abundant small-band-gap endohedral fullerene also appears to be a promising candidate for molecular electronics.

Experimental Section

High-purity graphite rods purchased from POCO were core-drilled (mass of the empty rod 6.3 g) and packed with a 1:1 mixture of graphite powder and Nd_2O_3 (1.4 g, total mass of carbon 7 g, neodymium oxide 0.7 g). After annealing at 1000 °C for 12 h, these rods were vaporized in a Kratschmer–Huffman arc reactor under a mixture of ammonia (20 mbar) and helium (200 mbar) using an arc current of 85 A. The soot collected from the arc reactor was then extracted with CS_2 in a sonicator for two hours. After removal of the solvent, the crude mixture was washed several times with ether until the solution was no longer colored. The solid residue was then redissolved in toluene. The $Nd_3N@C_{2n}$ cluster fullerenes were separated by HPLC using a Varian Pro Star model 210 and a semipreparative 10 × 250 mm Buckyprep-M column. Toluene was used as the mobile phase with a flow rate of 4 $mL\,min^{-1}$. MALDI-TOF mass spectrometry analysis was carried out using a Bruker Omni Flex. For the EDS analysis, the sample was deposited on a TEM grid and the spectrum was recorded on an HD-2000 STEM instrument equipped with an Oxford EDS system. The cyclic voltammetry experiment was carried out in a formal one-compartment cell connected to a BAS 100B workstation in a solution of *o*-DCB containing 0.05 M $[NBu_4][PF_6]$. A 2-mm-diameter glassy carbon disk was used as the working electrode. Ferrocene was added to the solution at the end of each experiment as an internal standard, and all the electrochemical potentials were referenced to its redox couple.

Received: August 1, 2007

Keywords: band gap · cage compounds · fullerenes · neodymium · nitrides

---

[1] a) H. Shinohara, *Rep. Prog. Phys.* **2000**, *63*, 843–892; b) *Endofullerenes: A New Family of Carbon Clusters* (Eds.: T. Akasaka, S. Nagase), Kluwer Academic Publishers, Dordrecht, **2002**.

[2] S. Stevenson, G. Rice, T. Glass, K. Harich, F. Cromer, M. R. Jordan, J. Craft, E. Hajdu, R. Bible, M. M. Olmstead, K. Maitra, A. J. Fisher, A. L. Balch, H. C. Dorn, *Nature* **1999**, *401*, 55–57.

[3] L. Dunsch, M. Krause, J. Noack, P. Georgi, *J. Phys. Chem. Solids* **2004**, *65*, 309.

[4] S. Stevenson, H. M. Lee, M. M. Olmstead, C. Kozikowski, P. Stevenson, A. L. Balch, *Chem. Eur. J.* **2002**, *8*, 4528.

[5] M. Krause, J. Wong, L. Dunsch, *Chem. Eur. J.* **2005**, *11*, 706 – 711.

[6] S. Stevenson, J. P. Phillips, J. E. Reid, M. M. Olmstead, S. P. Rath, A. L. Balch, *Chem. Commun.* **2004**, 2814 – 2815.

[7] M. Krause, L. Dunsch, *Angew. Chem.* **2005**, *117*, 1581 – 1584; *Angew. Chem. Int. Ed.* **2005**, *44*, 1557 – 1560.

[8] M. Wolf, K.-H. Müller, Y. Skourski, D. Eckert, P. Georgi, M. Krause, L. Dunsch, *Angew. Chem.* **2005**, *117*, 3371 – 3374; *Angew. Chem. Int. Ed.* **2005**, *44*, 3306 – 3309.

[9] S. Yang, L. Dunsch, *J. Phys. Chem. B* **2005**, *109*, 12320 – 12328.

[10] T. Zuo, C. M. Beavers, J. C. Duchamp, A. Campbell, H. C. Dorn, M. M. Olmstead, A. L. Balch, *J. Am. Chem. Soc.* **2007**, *129*, 2035 – 2043.

[11] a) S. Stevenson, P. W. Fowler, T. Heine, J. C. Duchamp, G. Rice, T. Glass, K. Harich, E. Hajdu, R. Bible, H. C. Dorn, *Nature* **2000**, *408*, 427; b) M. M. Olmstead, A. de Bettencourt-Dias, J. C. Duchamp, S. Stevenson, H. C. Dorn, A. L. Balch, *J. Am. Chem. Soc.* **2000**, *122*, 12220 – 12226; c) S. Yang, M. Kalbac, A. Popov, L. Dunsch, Lothar, *ChemPhysChem* **2006**, *7*, 1990 – 1995.

[12] J. M. Campanera, C. Bo, J. M. Poblet, *Angew. Chem.* **2005**, *117*, 7396 – 7399; *Angew. Chem. Int. Ed.* **2005**, *44*, 7230 – 7233.

[13] M. Krause, H. Kuzmany, P. Georgi, L. Dunsch, K. Vietze, G. Seifert, *J. Chem. Phys.* **2001**, *115*, 6596 – 6605.

[14] *CRC Handbook of Chemistry and Physics*, 81st ed. (Ed.: D. R. Lide), CRC, New York City, **2000**.

[15] a) C. M. Cardona, B. Elliott, L. Echegoyen, *J. Am. Chem. Soc.* **2006**, *128*, 6480 – 6485; b) S. Yang, M. Zalibera, P. Rapta, L. Dunsch, *Chem. Eur. J.* **2006**, *12*, 7848 – 7855; c) L. Zhang, N. Chen, L. Fan, C. Wang, S. Yang, *J. Electroanal. Chem.* **2007**, *608*, 15 – 21.

[16] L. Dunsch, S. Yang, *Phys. Chem. Chem. Phys.* **2007**, *9*, 3067 – 3081.